

## Preparation, characterization and determination of photocatalytic activity of MCM-41/ZnO and MCM-48/ZnO nanocomposites

Hamid Reza Pouretedal<sup>\*a</sup>, Mina Ahmadi<sup>b</sup>

<sup>a</sup> Faculty of Applied Chemistry, Malek-ashtar University of Technology, Shahin-Shahr, Iran.

<sup>b</sup> Department of Chemistry, Shahreza Branch, Islamic Azad University, Shahreza, Iran.

Received 7 August 2013; received in revised form 2 September 2013; accepted 25 September 2013

### ABSTRACT

The direct and indirect methods in solvent media and grinding method in a solvent-free media were used to prepare the MCM-41/ZnO and MCM-48/ZnO photocatalysts. The X-ray diffraction (XRD) patterns showed that zinc oxide nanoparticles were put into MCM-41 and MCM-48 substrates and there were ZnO crystallites as secondary phase in the extra framework of mesoporous materials. The decrease of surface areas, pore volume and average pore size of mesoporous materials with incorporation of ZnO nanoparticles were confirmed by N<sub>2</sub> adsorption and desorption isotherms. The FT-IR spectra showed an absorption peak at 490 cm<sup>-1</sup> that was related to formation of ZnO in the substrate of MCMs. The photocatalytic activity of MCM-41/ZnO and MCM-48/ZnO were studied in photodegradation reaction of Congo red as a dye pollutant. The photocatalysts of MCM-41/ZnO and MCM-48/ZnO which were prepared by grinding method showed the highest photocatalytic activity with pseudo first-order kinetic rate constants of 34.6 and 27.8×10<sup>-3</sup> min<sup>-1</sup>, respectively. The obtained results indicated complete incorporation of zinc ions in mesoporous material of MCMs in a solvent-free media. The elimination of solvent and facility of proposed method were the advantages of grinding method in preparation of MCM/ZnO photocatalyst.

**Keywords:** Mesoporous materials, Photocatalyst, MCM-41, MCM-48, ZnO, Congo red (CR).

### 1. Introduction

Mesoporous silica have been utilized in many fields of science and engineering including catalysis, adsorption, and separation, because they have uniform pore size, high surface area, and large pore volume [1-3]. It has been reported that mesoporous silicas formed by different templating agent exhibit different pore size, pore structure, and amount of surface hydroxyl group [3]. MCM-41, the hexagonal member of the M41S family of mesoporous molecular sieves has a regular honeycomb array of uniform cylindrical pores, which can be tailored to pores size ranging from 15-100 nm [4]. Besides their potential for catalytic conversion or adsorptive separation of bulky molecules, these mesoporous molecular sieves can also be used as host materials for specific molecules like porphyrins or other transition metal complexes [4,5]. A main drawback of these materials is their inactive chemical composition. Therefore, functionalization of surface is necessary to convert MCM-41 materials to those holding desirable

properties. The confinement of transition metal complexes within the constrained environment of ordered mesoporous oxides is an area of investigation that has developed since the discovery of M41S family [6].

MCM-48 is a member of the M41S mesoporous silica family. It consists of a cubic array with a three-dimensional pore network and has a high surface area and hydrothermal stability [7]. MCM-48 has already been used in many applications, including adsorption, ion exchange, catalysis, and so on [8]. In catalysis, the surface modification of M41S has been studied extensively. The incorporation of transition metals, such as, Ti, Cr, Fe or others, into M41S materials has been reported by a number of researchers [9,10]. The use of a solvent in incorporation process is seen in the most of researches. The aim of this research is study of preparation conditions of metal/M41S composite in the photocatalytic activity. It is expected that the preparation conditions is effective in the amount of metal incorporated in the channels of M41S mesoporous.

\* Corresponding author: E-mail: hr\_pouretedal@mut-es.ac.ir

As a well-known photocatalyst, ZnO has been paid much attention in the degradation and complete mineralization of environmental pollutants [11]. Since ZnO has approximately same band gap energy (3.2 eV) as TiO<sub>2</sub>, its photocatalytic capacity is anticipated to be similar to that of TiO<sub>2</sub>. Further studies have confirmed that ZnO exhibits more efficiency than TiO<sub>2</sub> in visible light photocatalytic degradation of some dyes, even in aqueous solution. Zinc oxide is an n-type semiconductor with many attractive features [12]. The synthesized ZnO was also shown to absorb more UV light than any other powders. This means that the high UV absorption efficiency leads to the generation of more electrons and holes. These electrons and holes are considered the main species involved in the photodegradation process [13,14].

In this study, the impregnation synthesis of zinc-doped MCM-41 and MCM-48 is studied by using direct and indirect solvothermal and grinding (without solvent) methods. A comparative study in structural properties of MCM-41/ZnO and MCM-48/ZnO materials is evaluated by XRD, FT-IR and BET methods. The photocatalytic activity of samples toward the photocatalytic degradation of Congo red (CR) in aqueous solution is studied.

## 2. Experimental

### 2.1. Synthesis of MCM-41 and MCM-48

Sodium silicate, cetyltrimethylammonium bromide (CTAB), tetramethylammonium hydroxide, tetraethyl orthosilicate (TEOS) and sodium hydroxide (all from Merck and Aldrich) were purchased from highest purity. The double distilled water was used to prepare the solutions.

MCM-41 was synthesized by dispersion of sodium silicate (2.5 g) in deionized water (18.24 ml) [5]. After stirring the components, the surfactant cetyltrimethylammonium bromide (CTAB) was added. The mixture of the reactants was stirred for 45 min at room temperature. During the vigorous stirring, an adequate amount of a 25% solution of tetramethylammonium hydroxide was added and the pH was adjusted at 10.5-11.0. The mixture was stirred at room temperature for 24 h, and then put into a teflon-lined autoclave and kept in it at 100°C for 3 days. The powder was recovered by filtration, and subsequently washed with acidic water-ethanol solution. It was dried in a vacuum oven and the obtained solid is calcined at 500°C for 4 h [15].

For synthesis of MCM-48, CTAB was dissolved in deionized water. Then sodium hydroxide and tetraethyl orthosilicate (TEOS) were added [7]. The molar composition of the gel was 1 M TEOS:0.25 M Na<sub>2</sub>O:0.65 M CTAB:0.62 M H<sub>2</sub>O. The solution was

stirred for about 1 h and then transferred into a polypropylene bottle and heated up to 100°C for 3 days. The product was filtered, and washed with water, and dried in air at ambient temperature. The dried product was finally calcined at 550°C for 6 h [7].

### 2.2. Synthesis of MCM-41/ZnO and MCM-48/ZnO

In indirect method, 0.1 g synthesized MCM-41 and/or MCM-48 material was added to 6.6 ml of 0.1 mol/L of zinc acetate (Zn(CH<sub>3</sub>COO)<sub>2</sub>·2H<sub>2</sub>O) solution and some polyethylene glycol as dispersant agent. The pH of obtained mixture was adjusted at 7-8 by addition of AR grade ammonium hydroxide and then, the mixture heated at 80°C for 2 h. After aging for 2 h, the colloid was filtered, and washed and then dried in a vacuum oven at 100°C for 2 h. The synthesized sample was calcined at 550°C for 5 h in air stream with a heating rate of 10°C/min. The MCM-41/ZnO and MCM-48/ZnO with 40% wt. of ZnO was obtained with cooling of materials as naturally to the ambient temperature [7,8].

MCM-41/ZnO and MCM-48/ZnO were prepared using a modified Stöber's synthesis at room temperature in a direct method. In a typical synthesis 1.2 g CTAB, 1.8 ml TEOS and 0.15 g of zinc acetate was taken in a polypropylene bottle. The deionized water and ethanol was added and stirred well until the dissolution of the metal precursor. The pH of mixture was controlled by addition of NH<sub>3</sub> solution. The obtained precipitate was filtered and washed with deionized water extensively. The solid was dried at 80°C for overnight in static air. The dried powder was ground finely and calcined in static air at 550°C to remove the surfactant molecules for 6 h [8].

In grinding procedure, 0.15 g of zinc acetate and 0.10 g of synthesized MCM-41 and/or MCM-48 separately, was taken in a mortar and grinding drastically at room temperature and finally, the obtained solid was calcined at 550°C in air for 3-4 h to remove the surfactant molecules [9].

The weight percent of ZnO was 40% in the prepared MCM-41/ZnO and MCM-48/ZnO samples.

### 2.3. Characterization of MCM-41/ZnO and MCM-48/ZnO

Nicolet Impact 400D FT-IR Spectrophotometer was used to prepare the IR-spectra of prepared photocatalysts in range 4000-400 cm<sup>-1</sup>. A Diffractometer Bruker D8 ADVANCE Germany with anode of Cu ( $\lambda=1.5406 \text{ \AA}$  of Cu K <sub>$\alpha$</sub> ) and filter of Ni was applied to record of X-ray diffraction (XRD) patterns of mesoporous MCM-41, MCM-48, MCM-41/ZnO and MCM-48/ZnO in the 2 $\theta$  ranges of 0.5 to 7° and 5 to 70°. N<sub>2</sub> adsorption isotherms of prepared photocatalysts were obtained by the B.E.T. method

using nitrogen as an adsorption gas at 77 K using a Belsorp Mini II instrument. Samples were out gassed at 300°C for 4 h prior to surface area measurements.

#### 2.4. Photocatalytic activity of prepared photocatalysts

Photocatalytic activity of MCM-41/ZnO and MCM-48/ZnO samples was studied in photodegradation reaction of Congo red (CR) at 25 °C and pH=7-8. The degradation was carried out in a Pyrex photoreactor contain a high pressure mercury lamp 70 W with maximum irradiation at wavelength of 332 nm. The degradation was performed at suitable time intervals at room temperature while the samples were stirred continuously. The photoreactor was filled with 25 mL of 50 mg/L of CR and 1.0 g/L of photocatalysts at pH of 7 [16]. The degradation efficiency (%D) was calculated from initial concentration ( $C_o$ ) and residual concentration ( $C_t$ ) of CR by spectrophotometric method at  $\lambda$  of 510 nm ( $\%D = [1 - (C_t/C_o)] \times 100$ ) in duration time 120 min with interval of 30 min. The adsorption/desorption of CR on the surface of photocatalysts solids was equilibrated at time 30 min in dark conditions.

The kinetic rate constant of degradation ( $k_{obs}$ ) was calculated by model of heterogeneous photocatalysis accordance to the Langmuir–Hinshelwood kinetic expression ( $\ln(C_o/C_t) = k_{obs}t$ ) [16,17].

### 3. Results and Discussion

#### 3.1. Characterization of prepared photocatalysts

The mesoporous materials of MCM-41 and MCM-48 and photocatalysts of MCM-41/ZnO and MCM-48/ZnO prepared by grinding method were characterized by XRD patterns, FT-IR spectra and the N<sub>2</sub> adsorption and desorption isotherms.

The XRD patterns of MCM-41 and MCM-41/ZnO at small-angle and wide-angle are shown in Fig. 1. The hexagonal ordered structured of MCM-41 were

confirmed by XRD patterns [1,6,7]. An intense diffraction peak (100) together with an additional peak (110) and a very weak peak (200), were observed in the small-angle XRD pattern of the prepared material of MCM-41 (Fig. 1a). It looks like that the (200) peak is not strong enough and also the diffraction peaks move to high angle and the peaks become weaker when the ZnO nanoparticles are doped in the MCM-41. These phenomena can be explained by the reduction of the tunnel size and the increase of ZnO nanoparticles in the pores and interaction of nanoparticles with the framework of MCM-41. The wide-angle of XRD patterns of MCM-41 and MCM-41/ZnO (Fig. 1b) only one diffusion peak was observed in the pattern of MCM-41, which indicates that the main substance of MCM-41 is amorphous silica. But when the ZnO nanoparticles were introduced into MCM-41, the peak of amorphous silica became weaker and the peaks of ZnO were appeared [18]. The peaks with  $2\theta$  values of 31, 34, 35.5, 47.5, 56.5, 62.5 and 68.5 show a hexagonal structure for ZnO nanoparticles in the framework of MCM-41 [19,20].

Fig. 2 shows the XRD patterns of MCM-48 and MCM-48/ZnO samples at small-angle and wide-angle. The XRD patterns of MCM-48 at small-angle showed a cubic ordered structured with the most intense diffraction peak (211) at  $2\theta=2.8^\circ$  [10]. This peak was an indicative for characterization of MCM-48. It was expected that the other low intensive diffraction peaks was seen in higher order at  $2\theta=3-6^\circ$  [2,3,10]. But, these peaks was not obviously seen in the pattern because very low intensity. Furthermore, the intensity of diffraction peak of MCM-48/ZnO decrease at small-angle, which was due to the gradual loss of long-range ordering when Zn doping. The diffraction peaks of ZnO in the wide-angle XRD pattern was appeared obviously which shows the content of ZnO in the channel (or in the extra framework) of sample with hexagonal structure [10].

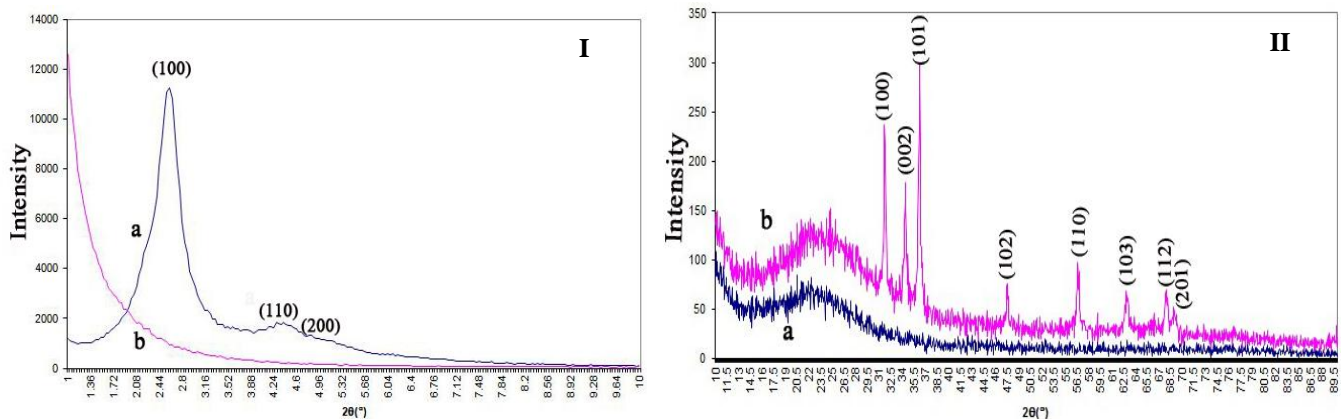


**Fig. 1.** (I) Small-angle and (II) wide-angle XRD patterns of samples (a) MCM-41 and (b) MCM-41/ZnO prepared by grinding method.

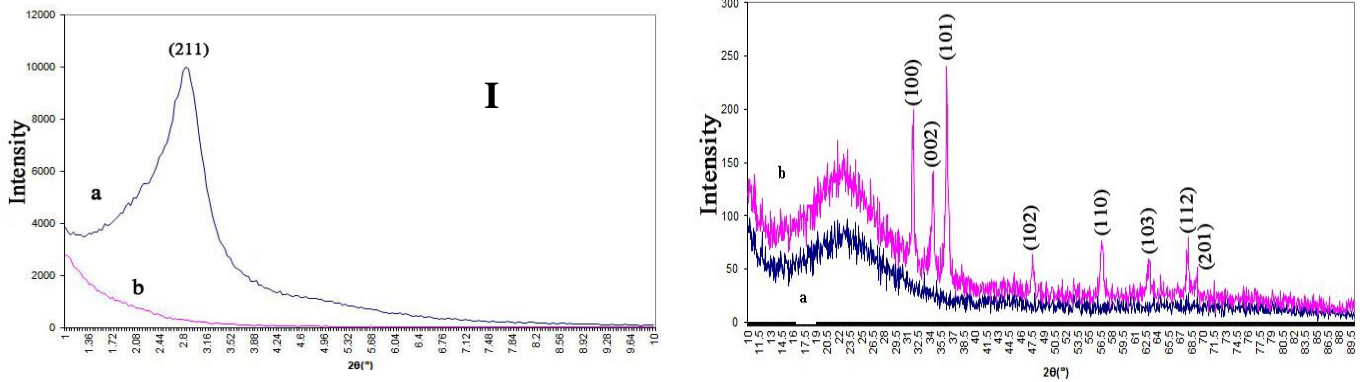


**Fig. 2.** (I) Small-angle and (II) wide-angle XRD patterns of samples (a) MCM-48 and (b) MCM-48/ZnO prepared by grinding method.

The FT-IR spectra of MCM-41 and MCM-41/ZnO are shown in Fig. 3. In the curve of MCM-41, the peaks at 3430-3440  $\text{cm}^{-1}$  were the stretching vibrating absorption peaks of O-H band in the surfaced hydroxyl and in the planar water. Three peaks, one at 1080  $\text{cm}^{-1}$  and another at 812 and 464  $\text{cm}^{-1}$ , were related to the framework of silicon, and they were the symmetry and asymmetry flexural vibrating peaks of Si-O-Si, respectively. In FT-IR spectra of MCM-41 and MCM-41/ZnO, there were some differences of the intensities of the peaks, which results from the doping of ZnO. An absorption peak at 490  $\text{cm}^{-1}$  was observed in the spectra of MCM-41/ZnO, and it indicates the formation of ZnO in the substrate [10,18].

The FT-IR absorption spectra of MCM-48 and MCM-48/ZnO samples are shown in Fig.4. The vibration absorption bands at 1230 and 1080  $\text{cm}^{-1}$  were due to the asymmetric vibration peaks of Si-O-Si absorption of silica framework. The band at 815  $\text{cm}^{-1}$  was due to the stretching vibration of silica, compared with the spectrum of MCM-48. The vibration band at 1630  $\text{cm}^{-1}$  for the MCM-48/ZnO sample can be considered as an indication of symmetric stretching vibration of carbonyl group of zinc acetate [18-20].

Brunauer-Emmett-Teller (BET) surface area analysis

and Barrett-Joyner-Halenda (BJH) pore size and volume analysis were used to characterize the prepared materials [21]. The BET data and BJH data of prepared materials are presented in Table 1. Surface areas (S), pore volume (P) and average pore size (D) were calculated by the BET and BJH models. The obtained results showed the ZnO loading could affect the mesoporous structure greatly, which has also been demonstrated by physicochemical properties of MCM-41/ZnO and MCM-48/ZnO [21,22]. The decrease of surface areas, pore volume and average pore size of mesoporous materials was seen with incorporation of ZnO nanoparticles in the framework of MCMs.

### 3.2. Photocatalytic degradation of Congo red (CR)

The photocatalytic activity of prepared photocatalysts was studied in Congo red photodegradation reaction. The obtained results include the degradation efficiency during 120 min of irradiation process, kinetic rate constants and Langmuir-Hinshelwood kinetic expression coefficients ( $R^2$ ), are collected in Table 2 and Fig. 5. The data were due to three replicate of experiments as well as uncertainty of results. The  $R^2$  values  $> 0.99$  show that the pseudo first-order kinetic can be used to determination of rate constants of CR degradation reaction catalyzed by photocatalysts.

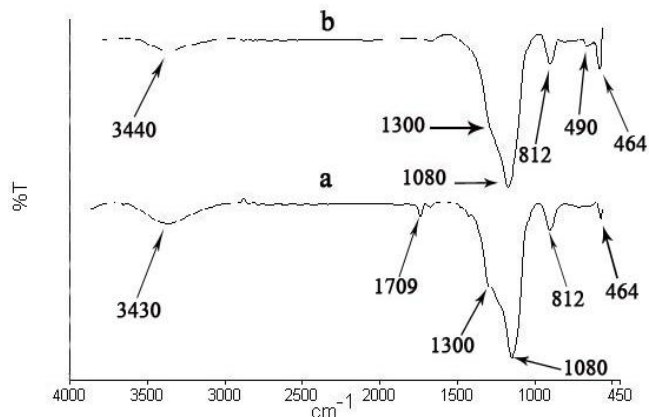


**Fig. 3.** FT-IR spectra of (a) MCM-41 and (b) MCM-41/ZnO prepared by grinding method.

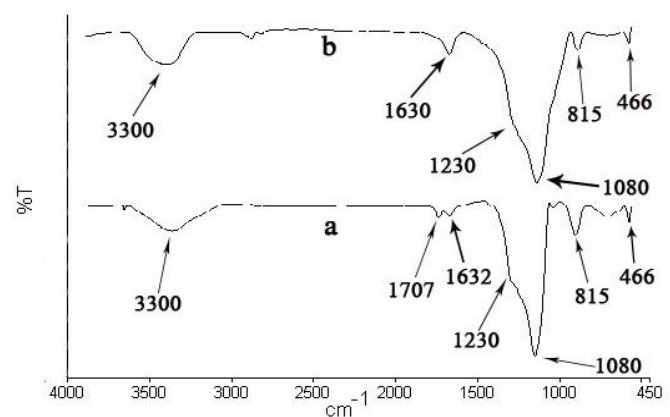


**Fig. 4.** FT-IR spectra of (a) MCM-48 and (b) MCM-48/ZnO prepared by grinding method.

**Table 1.** Textural properties of MCM-41, MCM-48 and MCM-41/ZnO and MCM-48/ZnO prepared by grinding method.

Sample	BET data			BJH data		
	S (m <sup>2</sup> /g)	P (cm <sup>3</sup> /g)	D (nm)	S (m <sup>2</sup> /g)	P (cm <sup>3</sup> /g)	D (nm)
MCM-41	895.0	0.850	2.230	845.6	0.765	2.126
MCM-41/ZnO	511.2	0.207	0.903	480.3	0.173	0.854
MCM-48	865.2	0.945	2.246	834.1	0.842	2.146
MCM-48/ZnO	489.3	0.245	0.967	466.1	0.184	0.987

The primary factor of photocatalytic degradation was the adsorption of CR onto the catalyst surface via the interaction of surface hydroxyl groups, particularly onto high surface area support, i. e. MCM-41 and MCM-48. In the other words, the adsorption of CR as an anionic dye on oxide surface was favored, leading to an increase of the dye concentration on the surface and facilitate the photocatalytic degradation of the dye investigated [14,19].

The presence of ZnO nanoparticles as photocatalyst on the mesoporous materials like MCM-41 and MCM-48, increase the photodegradation of CR dye under irradiation radiation [14,15]. Also, the hydroxyl groups on the surface of prepared catalysts act as an electron donor for photo-generated H<sup>+</sup>, and form active hydroxyl radicals (<sup>•</sup>OH) which attack CR.

The photocatalysts of MCM-41/ZnO and MCM-48/ZnO that prepared by grinding method show the highest photocatalytic activity (Table 2).

Apparently, the incorporation of zinc ions in the pores of mesoporous materials of MCMs was completed by grinding method versus direct and indirect methods [18-20]. Thus, the weight% of ZnO in mesoporous materials was increased by using of grinding method as a selective method in preparation of MCM/ZnO photocatalysts. However, a lot of zinc ions were become lost in preparation of MCM/ZnO by direct and indirect methods in a solvent medium. The amount of ZnO was measured by the digestion of prepared samples of ZnO/ MCM using AAS method. The amounts of ZnO were obtained 36.4, 25.9 and 21.8% in ZnO/MCM-41 and 35.3, 26.4 and 21.5% in ZnO/MCM-48 prepared by grinding, indirect and direct methods, respectively. Therefore, increasing of ZnO as a photocatalyst in MCM/ZnO samples caused to increasing in the photocatalytic activity of prepared samples.

The amount of CR degraded on the surface of the different photocatalysts showed the order of sequence:

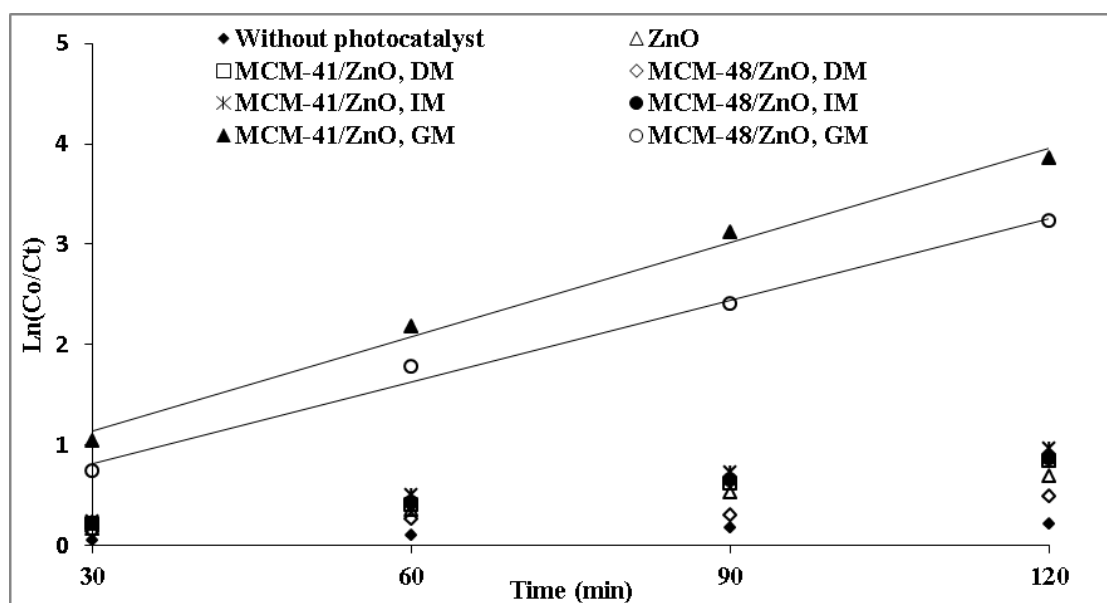


**Fig. 5.** The plots of  $\ln(C_0/C_t)$  versus time for MCM/ZnO photocatalysts prepared by direct method (DM), indirect method (IM) and grinding method (GM).

**Table 2.** The degradation of CR duration 120 min,  $k_{obs}$  and  $R^2$  values of photocatalytic process over ZnO, MCM-41/ZnO and MCM-48/ZnO samples. Standard deviations are related to  $n=3$ .

Catalysts	%D	$k_{obs} \times 10^{-3} \text{ (min}^{-1}\text{)}$	$R^2$
Without photocatalyst	22.9±1.2	1.9±0.2	0.9912
ZnO	43.2±2.1	5.7±0.4	0.9899
MCM-41/ZnO, direct method	48.6±1.9	6.9±0.2	0.9909
MCM-48/ZnO, direct method	39.2±2.8	4.2±0.3	0.9923
MCM-41/ZnO, indirect method	58.9±1.7	8.2±0.4	0.9897
MCM-48/ZnO, indirect method	53.4±2.5	7.2±0.2	0.9924
MCM-41/ZnO, grinding method	92.8±2.1	34.6±0.3	0.9901
MCM-48/ZnO, grinding method	86.4±1.1	27.8±0.3	0.9898

MCM-41/ZnO > MCM-48/ZnO > ZnO which could be directly related to the surface area that was available for adsorption. The data of Table 1 showed the more surface areas of MCM-41/ZnO versus MCM-48/ZnO. Therefore, good photodegradation was obtained over the MCMs/ZnO photocatalyst. The enhanced photocatalytic activity over the composite MCMs/ZnO was reflecting the beneficial adsorption properties of MCM-41 and MCM-48 [23,24]. Also, it was clear that the presence of zinc oxide in samples plays a key role in the photocatalytic reaction and these nanoparticles were the active sites in MCM/ZnO. The enhancements of degradation of CR may be due to the high dispersion of zinc oxide in the amorphous wall of MCM-41 and MCM-48 [25,26].

The higher activity of MCM-41/ZnO may be due to the hexagonal ordered structured compared to MCM-48 with cubic ordered structured. The hexagonal ordered structured of MCM-41 due to the higher dispersion of zinc ions on this sample [27,28].

As revealed by various studies on the photodegradation of azo dyes such as CR, the chromophore azo group was easily broken to generate  $N_2$  gas:



Also CR was oxidized by oxidative species and converted into fatty acids and finally into  $CO_2$ . Among the oxidative species,  $\cdot OH$  was the major oxidative transient and was known to react with benzene and azo moieties with high rate coefficients [12,14,29,30].

#### 4. Conclusions

MCM-41/ZnO and MCM-48/ZnO mesoporous materials can be synthesized successfully under ambient temperature by using grinding methods. The characterization of prepared samples shows that certain zinc cations had been incorporated in to the framework of MCM-41 and MCM-48. The MCM-41 and MCM-48 mesoporous materials indicate 2D hexagonal and 3D cubic structure, respectively. The doping of ZnO nanoparticles is due to decrease of surface area and pore volume of mesoporous materials. The MCM-41/ZnO and MCM-48/ZnO show the higher photoreactivity in CR degradation versus ZnO nanoparticles that is due to the higher surface area of photocatalyst. The hexagonal structure of MCM-41 with higher surface area and active sites and the existence of ZnO crystallinities as secondary phase in the extra framework of mesoporous are due to higher photocatalytic activity of MCM-41/ZnO versus MCM-48/ZnO. Finally, the photocatalytic activity of photocatalysts is increased with increasing the surface area and amount of incorporated semiconductor in a mesoporous substrate.

#### References

- [1] D. Kumar, K. Schumacher, C. du Fresne von Hohenesche, M. Grün, K.K. Unger, *Colloid Surface A*, 187–188 (2001) 109–116.
- [2] C. Danumah, S.M.J. Zaidi, N. Voyer, S. Giasson, S. Kaliaguine, *Mesoporous Molecular Sieves*, 117 (1998) 281–289.

- [3] R. Peng, D. Zhao, N. M. Dimitrijevic, T. Rajh, R.T. Koodali, *J. Phys. Chem., C* 116 (2012) 1605–1613.
- [4] M.A. Zanjanchi, A. Ebrahimian, M. Arvand, *J. Hazard. Mater.*, 175 (2010) 992–1000.
- [5] A. Corma, *Chem. Rev.*, 97 (1997) 2373–2420.
- [6] H. Yang, Y. Deng, C. Du, *Colloid Surface A*, 339 (2009) 111–117.
- [7] C. Le, L. Xiaoqin, *Chin. J. Chem. Eng.*, 16 (2008) 570–574.
- [8] M. Anpo, H. Yamashita, K. Ikeue, *Catal. Today*, 44 (1998) 327–332.
- [9] Y.F. Shao, L.Z. Wang, J.L. Zhang, *J. Photochem. Photobiol. A*, 180 (2006) 59–64.
- [10] K. Hadjiivanov, T. Tsoncheva, M. Dimitrov, C. Minchev, H. Knözinger, *Appl. Catal. A*, 241 (2003) 331–340.
- [11] F. Peng, H. Wang, H. Yu, S. Chen, *Mater. Res. Bulletin*, 41 (2006) 2123–2129.
- [12] D. Yu, R. Cai, Z. Liu, *Spectrochim. Acta A* 60 (2004) 1617–1624.
- [13] N. Daneshvar, S. Aber, M.S. Seyed Dorraji, A.R. Khataee, M.H. Rasoulifard, *Separation Purification Technol.*, 58 (2007) 91–98.
- [14] C. Hariharan, *Appl. Catal. A*, 304 (2006) 55–61.
- [15] X. Yang, Q. Guan, W. Li, *J. Environ. Manag.*, 92 (2011) 2939–2943.
- [16] H.R. Pouretedal, A. Kadkhodaie, *Chin. J. Catal.*, 31 (2010) 1328–1334.
- [17] A. Bagheri Ghomi, V. Ashayer, *Iran. J. Catal.*, 2 (2012) 135–140.
- [18] A. Sakthivel, S. E. Dapurkar, P. Selvam, *Catal. Lett.*, 77 (2001) 155–158.
- [19] S.H. Liu, H. Paul Wang, *International J. Hydrogen Energy*, 27 (2002) 859–862.
- [20] E. Caponetti, L. Pedone, M.L. Saladino, D. Chillura Martino, G. Nasillo, *Micropor. Mesopor. Mat.* 128 (2010) 101–107.
- [21] A.M. Busuioc, V. Meynen, E. Beyers, M. Mertens, P. Cool, N. Bilba and E.F. Vansant, *Appl. Catal. A*, 312 (2006) 153–164.
- [22] J. Sauer, F. Marlow, F. Schüth, *Phys. Chem. Chem. Phys.*, 3 (2001) 5579–5584.
- [23] P. Ji, J. Zhang, F. Chen, M. Anpo, *Ordered Mesoporous*, *J. Phys. Chem. C*, 112 (2008) 17809–17813.
- [24] S. Chaliha, K.G. Bhattacharyya, *Catal. Today*, 141 (2009) 225–233.
- [25] H. Yang, Y. Deng, C. Du, *Colloid Surface A*, 339 (2009) 111–117.
- [26] H.R. Pouretedal, M. Ahmadi, *Int. Nano Lett.* 2:10 (2012), doi:10.1186/2228-5326-2-10.
- [27] H.R. Pouretedal, S. Basati, *Iran. J. Catal.*, 2 (2012) 50–54.
- [28] S. Chaliha, K.G. Bhattacharyya, *J. Hazard. Mater.* 150 (2008) 728–736.
- [29] M. Alaei, A.R. Mahjoub, A. Rashidi, *Iran J. Chem. Chem. Eng.*, 31 (2012) 23–29.
- [30] H. Faghihian, A. Bahrani-fard, *Iran. J. Catal.* 1 (2011) 45–50.